RESEARCH ARTICLE

Semi-Intermittent Control Based Fixed/Predefined-Time Synchronization of Spatiotemporal Memristive Neural Networks

Ying Qiao[1], **Aminamuhan Abudireman**[1], **Abdujelil Abdurahman**[1,*] **and Jingjing You**[1]

[1] College of Mathematics and System Sciences, Xinjiang University, Urumqi 830046, China

Abstract

This article addresses the fixed-time (FXT) and predefined-time (PDT) synchronization issues of spatiotemporal memristive neural networks (MNNs). First, an aperiodic semi-intermittent control (ASIC) scheme is introduced to reduce the control costs. Then, some novel FXT/PDT synchronization criteria are obtained by using Guass's divergence theorem and by Lyapunov functional method. Finally, the feasibility of the theoretical results is confirmed through numerical simulations.

Keywords: memristor, spatiotemporal neural network, fixed-time/predefined-time synchronization, aperiodic semi-intermittent control.

1 Introduction

Over the past five decades, neural networks (NNs) have garnered significant interest due to their roles in computational learning, data analysis, and cryptographic image processing [1–4]. Since the simple non-uniform magnetic fields can cause electron drift, it necessitate the consideration of the diffusion phenomenon. This implies that the state of neurons changes not only with respect to the time variable but also with respect to the spatial variable. This phenomenon can be modeled using spatiotemporal NNs. In recent decades, the dynamic analysis of spatiotemporal NNs has become a focal point for many scholars [5–7].

The concept of memristors was first proposed by Professor Leon Chua in 1971 [8]. Memristor is a type of nonlinear resistive device that can reflect the relationship between magnetic flux and electric charge, and they have the ability to remember the amount of charge passed through them. Due to their similarity to biological synapses and their stronger memory capacity compared to traditional resistors, researchers have begun to replace resistors with memristors in artificial NNs to build MNNs [9]. In recent years, artificial NNs, especially MNNs, have been widely applied in various fields of science and engineering, associative memory, image processing and information storage[10, 11].

In practical engineering, control systems are often required to maintain stability within a finite time frame, such as robotic arms and spacecraft attitude tracking [12, 13]. It should be noted that the estimation of settling time (ST) in finite-time stability

Submitted: 08 August 2025
Accepted: 20 September 2025
Published: 17 November 2025

Vol. 1, **No.** 2, 2025.
10.62762/JNDA.2025.841722

***Corresponding author:**
✉ Abdujelil Abdurahman
abdujelil@xju.edu.cn

Citation
Qiao, Y., Abudireman, A., Abdurahman, A., & You, J. (2025). Semi-Intermittent Control Based Fixed/Predefined-Time Synchronization of Spatiotemporal Memristive Neural Networks. *Journal of Nonlinear Dynamics and Applications*, 1(2), 52–62.

is closely related to the system's initial values, which greatly limits practical applications' scope [14]. Consequently, the concept of FXT stability has emerged and garnered widespread attention, as it retains the rapid convergence and strong interference resistance of finite-time stability while avoiding dependence on initial values [15]. However, FXT stability also has certain drawbacks; the ST of FXT stability is still related to the parameters of the system under consideration, and its ST cannot be adjusted arbitrarily. Therefore, analyzing whether nonlinear systems can achieve stability within a specified time is a necessary task. This has led to the development of a new concept of stability, namely PDT stability [16, 17]. The convergence time of PDT stability can be bounded by any arbitrary time and is independent of the system's initial values and parameters.

With the development of FXT/PDT stability theories, FXT/PDT synchronization has been widely investigated [18–20]. Kong et al. [18] studied the FXT/PDT synchronization of discontinuous neutral competitive networks using adaptive control strategies. In [19], FXT/PDT synchronization of drive-response fuzzy inertial discontinuous NNs are achieved via a non-reduction method. Abdurahman et al. [20] investigated the FXT/PDT synchronization of a type of complex-valued BAM-NNs with stochastic perturbations by employing a non-separation method. Consider MNNs have extremely complex structures due to switching caused by memristor, the investigation of FXT/PDT synchronization control in MNNs is of great significance [4, 21].

Moreover, compared with continuous control, discontinuous control has the advantage of lower consumption and cost. Discontinuous control methods include impulsive control [22], event-triggered control [23], sampled-data control [24], and intermittent control [25, 26], among others. Intermittent control, as opposed to impulsive control, allows for the application of a limited number of successive control forces over a limited period of time. Intermittent control, compared to event triggering, is based on a time-triggered mechanism and does not require specific update conditions to be predefined. Among the intermittent controls, the aperiodic intermittent control is preferred due to its flexibility of time. This naturally leads to the question: can a aperiodic intermittent controller be designed to achieve FXT/PDT synchronization of spatiotemporal NNs?

Based on the considerations mentioned above, this paper investigates the FXT/PDT synchronization of spatiotemporal MNNs. Based on the newly designed ASIC, a set of direct and verifiable criteria have been developed to ensure the FXT/PDT synchronization of spatiotemporal MNNs. These criteria not only take into account the effects of spatial and temporal dynamics but also provide a quantitative assessment of the impacts of the control gains and control width of ASIC on synchronization analysis.

The remainder of the paper is structured as follows. Section 2 is the preparation which is used in this paper and gives the system of this paper. Section 3 the main focus of this paper, which is to design different ASIC schemes for FXT/PDT synchronization respectively. The stability of the system is proved through rigorous theoretical proofs. Section 4 verifies the correctness of the conclusions through numerical simulations. Finally conclude this paper and suggest future research directions.

Notations: $\mathbb{N}$, $\mathbb{R}$ and $\mathbb{Z}^+$ express the set of nonnegative integers, real numbers and positives integers. $\mathbb{R}^n$ stands for the set of n dimensional real vectors. $\Gamma = \{\rho||\rho_k| \leq h_k \text{ for } k = 1, 2, \cdots, l\}$ is a bounded compact set with smooth boundary $\partial\Gamma$ which mes$\Gamma \geq 0$ in $\mathbb{R}^l$, where $mes\Gamma$ is the measure of set Γ. Besides, $sign(\cdot)$ denotes the sign function.

2 Model description and preliminaries

Consider the spatiotemporal MNNs as follows

$$\begin{aligned}\frac{\partial z_\ell(t,\rho)}{\partial t} =& \sum_{k=1}^{l} d_{\ell k}\frac{\partial^2 z_\ell(t,\rho)}{\partial \rho_k^2} - c_\ell z_\ell(t,\rho) \\ &+ \sum_{n=1}^{p} a_{\ell n}(z_\ell(t,\rho))f_n\left(z_j(t,\rho)\right) + I_\ell,\end{aligned} \tag{1}$$

where $\ell \in \mathcal{I} \triangleq \{1, 2, \ldots, p\}$, $\rho = (\rho_1, \rho_2, \ldots, \rho_l)^T \in \Gamma \subset \mathbb{R}^l$; $z_\ell(t,\rho)$ represents the state variable of the ℓ-th neuron at time t; $c_\ell > 0$ denotes the self-inhibition coefficient of the neuron; $a_{\ell n}(z_\ell(t,\rho))$ is the connection weight; $f_n(\cdot)$ represents the activation function; $d_\ell \geq 0$ denotes the transmission diffusion coefficient along the ℓ-th neuron; and I_ℓ represents the external input to the ℓ-th neuron.

The initial conditions and Dirichlet boundary conditions for system (1) are:

$$\begin{cases} z_\ell(t_0,\rho) = \eta_\ell(\rho), & \rho \in \Gamma, \\ z_\ell(t,\rho) = 0, & (t,\rho) \in [t_0, +\infty) \times \partial\Gamma, \end{cases} \tag{2}$$

where $\eta_\ell(\rho)$ is a bounded continuous function on the space Γ. The state of the system (1) satisfies

$$a_{\ell n}\left(z_\ell(t,\rho)\right)=\begin{cases}\hat{a}_{\ell n}, & sign_{\ell n}\frac{\partial f_n(z_n(t,\rho))}{\partial t}-\frac{\partial z_\ell(t,\rho)}{\partial t}<0,\\ *, & sign_{\ell n}\frac{\partial f_n(z_n(t,\rho))}{\partial t}-\frac{\partial z_\ell(t,\rho)}{\partial t}=0,\\ \check{a}_{\ell n}, & sign_{\ell n}\frac{\partial f_n(z_n(t,\rho))}{\partial t}-\frac{\partial z_\ell(t,\rho)}{\partial t}>0,\end{cases}\tag{3}$$

where $\hat{a}_{\ell n}$ and $\check{a}_{\ell n}$ are constants and $*$ denotes unchanged. The phrase remains unchanged means that the memristor retains its current value. Therefore, system (1) can be expressed as

$$\begin{aligned}\frac{\partial z_\ell(t,\rho)}{\partial t}\in&\sum_{k=1}^{l}d_{\ell k}\frac{\partial^2 z_\ell(t,\rho)}{\partial\rho_k^2}-c_\ell z_\ell(t,\rho)\\&+\sum_{n=1}^{n}co\{\hat{a}_{\ell n},\check{a}_{\ell n}\}f_n\left(z_n(t,\rho)\right)+I_\ell.\end{aligned}\tag{4}$$

Based on set-valued mapping and differential inclusion theory, there exist $\bar{a}_{\ell n}\in co\{\hat{a}_{\ell n},\check{a}_{\ell n}\}$ such taht

$$\begin{aligned}\frac{\partial z_\ell(t,\rho)}{\partial t}=&\sum_{k=1}^{l}d_{\ell k}\frac{\partial^2 z_\ell(t,\rho)}{\partial\rho_k^2}-c_\ell z_\ell(t,\rho)\\&+\sum_{n=1}^{p}\bar{a}_{\ell n}f_n\left(z_n(t,\rho)\right)+I_\ell.\end{aligned}\tag{5}$$

Taking the system (1) as the driving system, its corresponding response system is

$$\begin{aligned}\frac{\partial \tilde{z}_\ell(t,\rho)}{\partial t}=&\sum_{k=1}^{l}d_{\ell k}\frac{\partial^2 \tilde{z}_\ell(t,\rho)}{\partial\rho_k^2}-c_\ell \tilde{z}_\ell(t,\rho)\\&+\sum_{n=1}^{p}a_{\ell n}(\tilde{z}_\ell(t,\rho))f_n\left(\tilde{z}_n(t,\rho)\right)+I_\ell+u_\ell(t,\rho),\end{aligned}\tag{6}$$

where $u_\ell(t,\rho)$ is the controller to be designed. The initial conditions and Dirichlet boundary conditions for system (6) are

$$\begin{cases}\tilde{z}_\ell(t_0,\rho)=\phi_\ell(\rho), & \rho\in\Gamma,\\ \tilde{z}_\ell(t,\rho)=0, & (t,\rho)\in[t_0,+\infty)\times\partial\Gamma,\end{cases}\tag{7}$$

where $u_\ell(t,\rho)$ is the controller to be designed. Similarly, based on set-valued mapping and differential inclusion theory, the exist $\underline{a}_{\ell n}\in \mathrm{co}\{\hat{a}_{\ell n},\check{a}_{\ell n}\}$ such that system (6) can be represented as

$$\begin{aligned}\frac{\partial \tilde{z}_\ell(t,\rho)}{\partial t}=&\sum_{k=1}^{l}d_{\ell k}\frac{\partial^2 \tilde{z}_\ell(t,\rho)}{\partial\rho_k^2}-c_\ell \tilde{z}_\ell(t,\rho)\\&+\sum_{n=1}^{p}\underline{a}_{\ell n}f_n\left(\tilde{z}_n(t,\rho)\right)+I_\ell+u_\ell(t,\rho).\end{aligned}\tag{8}$$

Remark 1 In the realm of NNs synchronization research, the study of partial differential NN models and MMNs has garnered significant attention from the academic community. Moreover, this research encompasses the advancements of state-dependent MNNs across various synchronization types. However, the existing literature [27] and [28] have not sufficiently taken into account the influence of spatial factors on state variables, which may impede the models' precision and applicability in capturing the dynamic behaviors of complex systems. In view of this, the model proposed in this study will further integrate spatial effects based on prior research, aiming to develop a more precise and comprehensive MNN model.

Definition 1 ([28]) If there exists a time T^* which is independent of the initial values, such that for all $\ell=1,2,\ldots,p$

$$\lim_{t\to T^*}\|\tilde{z}_\ell(t,\rho)-z_\ell(t,\rho)\|=0$$
$$\text{and}\quad \|\tilde{z}_\ell(t,\rho)-z_\ell(t,\rho)\|=0,\forall t\geq T^*,$$

then the spatiotemporal MNNs (1) and (6) are said to achieve fixed-time synchronization. Furthermore, if there exists a specified constant $T_c>0$ such that for all $t\geq T_c$, $\lim_{t\to T_c}\|\tilde{z}_\ell(t,\rho)-z_\ell(t,\rho)\|=0$, and T_c is completely independent of the system parameters, then the systems (1) and (6) are said to achieve PDT synchronization.

Assumption 1 In system (1), the activation functions f_n satisfy the Lipschitz condition, i.e., there exist constants $l_n>0$ such that

$$|f_n(z_1)-f_n(z_2)|\leq l_n|z_1-z_2|,\quad \forall z_1,z_2\in\mathbb{R}.\tag{9}$$

Moreover, the activation functions are bounded; that is, there exist constants $F_n>0$ such that

$$|f_n(z)|\leq F_n,\quad \forall z\in\mathbb{R}.\tag{10}$$

where $z_1,z_2\in\mathbb{R}$, $n=1,2,\ldots,p$.

Lemma 1 ([29]) Let Γ be cube $|\rho_k|<h_k$, $z(\rho)$ is a real-valued function belonging to $C^1(\Gamma)$ which vanishes on the boundary $\partial\Gamma$ of Γ, i.e., $z(\rho)|_{\partial\Gamma}=0$. Then

$$\int_\Gamma z^2(\rho)\mathrm{d}\rho\leq h_k^2\int_\Gamma\left|\frac{\partial z(\rho)}{\partial\rho_k}\right|^2\mathrm{d}\rho,\ k=1,2,...,l.$$

Lemma 2 ([25]) Assume that the differentiable and non-negative function $V(t)$ satisfies

$$\dot{V}(t)\leq\begin{cases}k_1V(t)-\lambda V^\mu(t)-\gamma V^\nu(t), & t\in[t_\chi,\sigma_\chi),\\ k_2V(t), & t\in[\sigma_\chi,t_{\chi+1}),\end{cases}\tag{11}$$

where $t_\chi \geq 0$, $\chi \in \mathbb{N}$, $\mu > 1$, $0 < \nu < 1$, and $\lambda, \gamma > 0$, k_1, $k_2 \neq 0$, and $k_1 \leq min\{\lambda, \gamma\}$. If there exists $\varphi = \lim_{\chi\to\infty} sup\frac{t_{\chi+1}-\sigma_\chi}{t_{\chi+1}-t_\chi}$, such that $|k_1| - (|k_1| + |k_2|)\varphi > 0$ holds, then $V(t) = 0$ for all $t \geq T^*$, and T^* satisfies

$$T^* = \frac{In(|k_1|\lambda^{-\varrho}\gamma^{\varpi} + 1)}{(|k_1| - (|k_1| + |k_2|)\varphi)}\left(\frac{1}{\mu - 1} + \frac{1}{1 - \nu}\right),$$

where $\varrho = \frac{1-\nu}{\mu-\nu}$, $\varpi = \frac{1-\mu}{\mu-\nu}$.

Lemma 3 ([26]) Assume that the differentiable and non-negative function $V(t)$ satisfies

$$\dot{V}(t) \leq \begin{cases} k_1 V(t) - \frac{T_0}{T_c}\lambda V^{\mu}(t) - \frac{T_0}{T_c}\gamma V^{\nu}(t), t \in [t_\chi, s_\chi), \\ k_2 V(t), \qquad\qquad\qquad\qquad t \in [s_\chi, t_{\chi+1}), \end{cases} \tag{12}$$

where $t_\chi \geq 0$, $\chi \in \mathbb{N}$, $\mu > 1$, $0 < \nu < 1$, and $\lambda, \gamma > 0$, k_1, $k_2 \neq 0$, $T_c > 0$ is an arbitrary given positive constant that satisfies $T_c \leq T_0$,

$$T_0 = \frac{|k_1|\lambda^{-\varrho}\gamma^{\varpi}}{(|k_1| - (|k_1| + |k_2|)\varphi)}\left(\frac{1}{\mu - 1} + \frac{1}{1 - \nu}\right),$$

where $\varrho = \frac{1-\nu}{\mu-\nu}$, $\varpi = \frac{1-\mu}{\mu-\nu}$. If there exists $\varphi = \lim_{\chi\to\infty} sup\frac{t_{\chi+1}-\sigma_\chi}{t_{\chi+1}-t_\chi}$, such that $|k_1| - (|k_1| + |k_2|)\varphi > 0$ holds, then $V(t) = 0$ for all $t \geq T_c$.

3 Main results

3.1 FXT synchronization

In this section, we derive the sufficient conditions for the drive system (1) and the response system (6) to achieve FXT synchronization. The error system is

$$\begin{aligned} \frac{\partial e_\ell(t,\rho)}{\partial t} =& \sum_{k=1}^{l} d_{\ell k}\frac{\partial^2 e_\ell(t,\rho)}{\partial \rho_k^2} - c_\ell e_\ell(t,\rho) \\ &+ \sum_{n=1}^{p} \underline{a}_{\ell n} f_n\left(\tilde{z}_n(t,\rho)\right) - \sum_{n=1}^{p} \bar{a}_{\ell n} f_n\left(z_n(t,\rho)\right) \\ &+ u_\ell(t,\rho) \\ =& \sum_{k=1}^{l} d_{\ell k}\frac{\partial^2 e_\ell(t,\rho)}{\partial \rho_k^2} - c_\ell e_\ell(t,\rho) \\ &+ \sum_{n=1}^{p} \underline{a}_{\ell n}\left[f_n\left(\tilde{z}_n(t,\rho)\right) - f_n\left(z_n(t,\rho)\right)\right] \\ &+ \sum_{n=1}^{p}\left[\underline{a}_{\ell n} - \bar{a}_{\ell n}\right] f_n\left(z_n(t,\rho)\right) + u_\ell(t,\rho), \end{aligned} \tag{13}$$

where $e_\ell(t,\rho) = \tilde{z}_\ell(t,\rho) - z_\ell(t,\rho)$.

Firstly, design the following ASIC

$$u_\ell(t,\rho) = \begin{cases} -\kappa_\ell sign(e_\ell(t,\rho)) - \alpha_\ell \hat{e}^{-1}(t) e_\ell(t,\rho) \\ -\beta_\ell \hat{e}^{2(q-1)}(t) e_\ell(t,\rho), \qquad t \in [t_\chi, s_\chi), \\ -\kappa_\ell sign(e_\ell(t,\rho)), \qquad t \in [s_\chi, t_{\chi+1}), \end{cases} \tag{14}$$

where $q > 1$, κ_ℓ, α_ℓ, $\beta_\ell > 0$, and $\hat{e}(t) = \left(\int_\Gamma \sum_{\ell=1}^{p} e_\ell^2(t,\rho)\,\mathrm{d}\rho\right)^{\frac{1}{2}}$.
Denote

$$N_\ell = -\zeta_\ell - 2c_\ell + \sum_{n=1}^{p}(|\underline{a}_{\ell n}|l_n + |\underline{a}_{n\ell}|l_\ell),$$

where $\zeta_\ell = \sum_{k=1}^{l} \frac{2d_{\ell k}}{h_k^2}$.

Remark 2. ASIC substantially saves the energy consumption by simplifying the controller during resting intervals. It also requires no fixed control periods and can adapt to dynamic system changes; and effectively accommodates non-uniform diffusion characteristics in spatiotemporal systems without predefined periodic constraints. These characteristics make ASIC particularly suitable for synchronization control of spatiotemporal MNNs.

Theorem 1 Under Assumption 1, if the system parameters satisfy $\kappa_\ell \geq \sum_{n=1}^{p} d_{\ell n}^a F_n$ and $N = \max_{1\leq\ell\leq p}\{N_\ell\} \leq \min\{\lambda, \gamma\}$, then the drive system (1) and response system (6) achieve FXT synchronization, with a ST of $T^* \triangleq \frac{\ln(|k_1|\lambda^{-\varrho}\gamma^{\varpi}+1)}{(|k_1|-(|k_1|+|k_2|)\varphi)}\left(\frac{1}{\mu-1} - \frac{1}{1-\nu}\right)$, where $\varpi = \frac{1-\mu}{\mu-\nu}$, $\varrho = \frac{1-\nu}{\mu-\nu}$, $\mu = q$, $\nu = \frac{1}{2}$, $k_1 = k_2 = N$, $\gamma = 2\min_{1\leq\ell\leq p}\{\alpha_\ell\}$, and $\lambda = 2\min_{1\leq\ell\leq p}\{\beta_\ell\}$.

Proof. The Lyapunov functional can be selected as:

$$V(t) = \int_\Gamma \sum_{\ell=1}^{p} e_\ell^2(t,\rho)\mathrm{d}\rho. \tag{15}$$

When $t \in [t_\chi, s_\chi)$, calculating Dini derivative of $V(t)$ along the error system (13), we obtain

$$\begin{aligned} D^+V(t) = \int_\Gamma \Bigg\{ \sum_{\ell=1}^{p} 2e_\ell(t,\rho)\Bigg[\sum_{k=1}^{l} d_{\ell k}\frac{\partial^2 e_\ell(t,\rho)}{\partial \rho_k^2} \\ - c_\ell e_\ell(t,\rho) + \sum_{n=1}^{p} \underline{a}_{\ell n}[f_n(\tilde{z}_n(t,\rho)) \\ - f_n(z_n(t,\rho))] + \sum_{n=1}^{p}[\underline{a}_{\ell n} - \bar{a}_{\ell n}]f_n(z_n(t,\rho)) \\ - \kappa_\ell sign(e_\ell(t,\rho)) - \alpha_\ell \hat{e}^{-1}(t) e_\ell(t,\rho) \end{aligned}$$

$$
\begin{aligned}
&- \beta_\ell \hat{e}^{2(q-1)}(t) e_\ell(t,\rho)\Big]\Big\}\mathrm{d}\rho \\
&\le \int_\Gamma \Big\{ \sum_{\ell=1}^{p}\sum_{k=1}^{l} 2e_\ell(t,\rho) d_{\ell k} \frac{\partial^2 e_\ell(t,\rho)}{\partial \rho_k^2} \\
&- \sum_{\ell=1}^{p} 2c_\ell e_\ell^2(t,\rho) \\
&+ \sum_{\ell=1}^{p}\sum_{n=1}^{p} 2e_\ell(t,\rho)\underline{a}_{\ell n} g_n(e_n(t,\rho)) \\
&+ \sum_{\ell=1}^{p}\sum_{n=1}^{p} 2d_{\ell n}^a F_n |e_\ell(t,\rho)| - \sum_{\ell=1}^{p} 2\kappa_\ell |e_\ell(t,\rho)| \\
&- \sum_{\ell=1}^{p} 2\alpha_\ell e_\ell(t,\rho)\hat{e}^{-1}(t) e_\ell(t,\rho) \\
&- \sum_{\ell=1}^{p} 2\beta_\ell e_\ell(t,\rho)\hat{e}^{2(q-1)}(t) e_\ell(t,\rho)\Big\}\mathrm{d}\rho,
\end{aligned} \tag{16}
$$

where $g_n(e_n(t,\rho)) = f_n(\tilde{z}_n(t,\rho)) - f_n(z_n(t,\rho))$, $d_{\ell n}^a = \underline{a}_{\ell n} - \overline{a}_{\ell n}$, and $|f_n(z_\ell)| \le F_n$.

According to the Gauss's divergence theorem and the boundary conditions (2) and (7), it can be obtained that

$$
\begin{aligned}
&\int_\Gamma \sum_{\ell=1}^{p} 2e_\ell(t,\rho) \sum_{k=1}^{l} d_{\ell k} \frac{\partial^2 e_\ell(t,\rho)}{\partial \rho_k^2}\mathrm{d}\rho \\
&= \int_\Gamma \sum_{\ell=1}^{p} 2e_\ell(t,\rho)\left[\nabla \cdot \left(d_{\ell k}\frac{\partial e_\ell(t,\rho)}{\partial \rho_k}\right)_{k=1}^{l}\right]\mathrm{d}\rho \\
&= \int_\Gamma 2\sum_{\ell=1}^{p}\left[\nabla \cdot \left(e_\ell(t,\rho) d_{\ell k}\frac{\partial e_\ell(t,\rho)}{\partial \rho_k}\right)_{k=1}^{l}\right. \\
&\quad \left. - \nabla e_\ell(t,\rho) \cdot \left(d_{\ell k}\frac{\partial e_\ell(t,\rho)}{\partial \rho_k}\right)_{k=1}^{l}\right]\mathrm{d}\rho \\
&= \int_{\partial\Gamma} 2\sum_{\ell=1}^{p}\left[\left(d_{\ell k} e_\ell(t,\rho)\frac{\partial e_\ell(t,\rho)}{\partial \rho_k}\right)_{k=1}^{l}\cdot \mathbf{n}\right]\mathrm{d}\rho \\
&\quad - \int_\Gamma 2\sum_{\ell=1}^{p}\sum_{k=1}^{l} d_{\ell k}\left(\frac{\partial e_\ell(t,\rho)}{\partial \rho_k}\right)^2\mathrm{d}\rho \\
&= - \int_\Gamma 2\sum_{\ell=1}^{p}\sum_{k=1}^{l} d_{\ell k}\left(\frac{\partial e_\ell(t,\rho)}{\partial \rho_k}\right)^2\mathrm{d}\rho,
\end{aligned} \tag{17}
$$

where $\langle\cdot\rangle$ denotes the inner product, $\mathbf{n}$ is the unit outward normal to the boundary $\partial\Gamma$, $\nabla = \left(\frac{\partial}{\partial\rho_1},\ldots,\frac{\partial}{\partial\rho_l}\right)$ is the gradient operator, and

$$
\left(\frac{\partial e_\ell(t,\rho)}{\partial \rho_k}\right)_{k=1}^{l} = \left(\frac{\partial e_\ell(t,\rho)}{\partial \rho_1}, \frac{\partial e_\ell(t,\rho)}{\partial \rho_2}, \ldots, \frac{\partial e_\ell(t,\rho)}{\partial \rho_l}\right)^T.
$$

According to Lemma 1, we can obtain

$$
\begin{aligned}
&- \int_\Gamma 2\sum_{\ell=1}^{p}\sum_{k=1}^{l} d_{\ell k}\left(\frac{\partial e_\ell(t,\rho)}{\partial \rho_k}\right)^2\mathrm{d}\rho \\
&\le \int_\Gamma \sum_{\ell=1}^{p} -\zeta_\ell e_\ell^2(t,\rho)\mathrm{d}\rho.
\end{aligned} \tag{18}
$$

where $\zeta_\ell = \sum_{k=1}^{l}\frac{2d_{\ell k}}{h_k^2}$.

According to the Lipschitz condition, we have

$$
\begin{aligned}
&\sum_{\ell=1}^{p}\sum_{n=1}^{p} 2e_\ell(t,\rho)\underline{a}_{\ell n} g_n(e_n(t,\rho)) \\
&\le \sum_{\ell=1}^{p}\sum_{n=1}^{p} 2|e_\ell(t,\rho)||\underline{a}_{\ell n}||g_n(e_n(t,\rho))| \\
&\le \sum_{\ell=1}^{p}\sum_{n=1}^{p}(|\underline{a}_{\ell n}| l_n + |\underline{a}_{n\ell}| l_\ell) e_\ell^2(t,\rho).
\end{aligned} \tag{19}
$$

According to the definition of $\hat{e}(t)$, we can obtain

$$
\begin{aligned}
&- \int_\Gamma \sum_{\ell=1}^{p} 2\alpha_\ell e_\ell(t,\rho)\hat{e}^{-1}(t) e_\ell(t,\rho)\mathrm{d}\rho \\
&= -2\hat{e}^{-1}(t)\int_\Gamma \sum_{\ell=1}^{p}\alpha_\ell e_\ell^2(t,\rho)\mathrm{d}\rho \\
&\le -2\min_{1\le\ell\le p}\{\alpha_\ell\}\,\hat{e}^{-1}(t)\hat{e}^2(t) \\
&= -2\min_{1\le\ell\le p}\{\alpha_\ell\}\,V^{\frac{1}{2}}(t),
\end{aligned} \tag{20}
$$

$$
\begin{aligned}
&- \int_\Gamma \sum_{\ell=1}^{p} 2\beta_\ell e_\ell(t,\rho)\hat{e}^{2(q-1)}(t) e_\ell(t,\rho)\mathrm{d}\rho \\
&= -2\hat{e}^{2(q-1)}(t)\int_\Gamma \sum_{\ell=1}^{p}\beta_\ell e_\ell^2(t,\rho)\mathrm{d}\rho \\
&\le -2\min_{1\le\ell\le p}\{\beta_\ell\}\,\hat{e}^{2(q-1)}(t)\hat{e}^2(t) \\
&= -2\min_{1\le\ell\le p}\{\beta_\ell\}\,V^q(t).
\end{aligned} \tag{21}
$$

Substituting Eqs (18)-(21) into (16), we can obtain

$$
\begin{aligned}
\dot{V}(t) \le &\int_\Gamma \sum_{\ell=1}^{p}\Big[-\zeta_\ell - 2c_\ell + \sum_{n=1}^{p}(|\underline{a}_{\ell n}| l_n + |\underline{a}_{n\ell}| l_\ell)\Big] \\
&\times e_\ell^2(t,\rho)\mathrm{d}\rho + \int_\Gamma\Big(\sum_{\ell=1}^{p} 2\Big(\sum_{n=1}^{p} d_{\ell n}^a F_n - \kappa_\ell\Big)\Big)|e_\ell(t,\rho)|\mathrm{d}\rho \\
&- 2\min_{1\le\ell\le p}\{\alpha_\ell\}\,V^{\frac{1}{2}}(t) - 2\min_{1\le\ell\le p}\{\beta_\ell\}\,V^q(t) \\
\le &NV(t) - \gamma V^\nu(t) - \lambda V^\mu(t).
\end{aligned} \tag{22}
$$

When $t \in [s_\chi, t_{\chi+1})$

$$\begin{aligned}\dot{V}(t) \leq & \int_\Gamma \sum_{\ell=1}^{p} \Big[-\zeta_\ell - 2c_\ell + \sum_{n=1}^{p} (|\underline{a}_{\ell n}| l_n + |\underline{a}_{n\ell}| l_\ell) \Big] \\ & \times e_\ell^2(t,\rho) \mathrm{d}\rho + \int_\Gamma \Big(\sum_{\ell=1}^{p} 2 \big(\sum_{n=1}^{p} d_{\ell n}^a F_n - \kappa_\ell \big) \Big) |e_\ell(t,\rho)| \mathrm{d}\rho \\ \leq & NV(t). \end{aligned} \tag{23}$$

Combining (22) and (23), it follows that

$$\dot{V}(t) \leq \begin{cases} k_1 V(t) - \lambda V^\mu(t) - \gamma V^\nu(t), & t \in [t_\chi, s_\chi), \\ k_2 V(t), & t \in [s_\chi, t_{\chi+1}), \end{cases} \tag{24}$$

Here, $\varpi = \frac{1-\mu}{\mu-\nu}$, $\varrho = \frac{1-\nu}{\mu-\nu}$, $\mu = q > 1$, $\nu = \frac{1}{2}$, $k_1 = k_2 = N = \max\limits_{1\leq \ell \leq p} \{N_\ell\}$, $\gamma = 2 \min\limits_{1\leq \ell \leq p} \{\alpha_\ell\}$, and $\lambda = 2 \min\limits_{1\leq \ell \leq p} \{\beta_\ell\}$. Therefore, according to Lemma 2, the drive system (1) and the response system (6) achieve FXT synchronization with the ST T^*.

Remark 3. The proposed control framework in this paper can be extended to study the FXT synchronization of stochastic, fuzzy, fractional-order and other types of NNs, though each extension requires specific adaptations. For fractional-order systems, this entails adopting fractional Lyapunov methods and revising ST criteria. For stochastic systems, it involves using Itô's formula and analyzing noise impacts. The method also applies to inertial, complex-valued, and time-delayed networks via techniques such as non-reduction methods and Lyapunov-Krasovskii functionals.

3.2 PDT synchronization

In this section, by designing a novel controller, the PDT synchronization between the drive-response systems (1) and (6) is achieved. First, the PDT ASIC in system (6) is designed as

$$u_\ell(t,\rho) = \begin{cases} -\kappa_\ell sign(e_\ell(t,\rho)) - \frac{T_0}{T_c} \alpha_\ell \hat{e}^{-1}(t) e_\ell(t,\rho) \\ -\frac{T_0}{T_c} \beta_\ell \hat{e}^{2(q-1)}(t) e_\ell(t,\rho), & t \in [t_\chi, s_\chi), \\ -\kappa_\ell sign(e_\ell(t,\rho)), & t \in [s_\chi, t_{\chi+1}), \end{cases} \tag{25}$$

where $q > 1$, κ_ℓ, α_ℓ, $\beta_\ell > 0$, $\hat{e}(t) = \big(\int_\Gamma \sum_{\ell=1}^{p} e_\ell^2(t,\rho) \mathrm{d}\rho \big)^{\frac{1}{2}}$.
Denote

$$N_\ell = -\zeta_\ell - 2c_\ell + \sum_{n=1}^{p} (|\underline{a}_{\ell n}| l_n + |\underline{a}_{n\ell}| l_\ell),$$

where $\zeta_\ell = \sum_{k=1}^{l} \frac{2d_{\ell k}}{h_k^2}$.

Theorem 2 Under Assumption 1, if the system parameters satisfy $\kappa_\ell \geq \sum_{n=1}^{p} d_{\ell n}^a F_n$ and $N = \max_{1\leq \ell \leq p} \{N_\ell\} \leq \min\{\frac{T_0}{T_c}\lambda, \frac{T_0}{T_c}\gamma\}$, then the drive-response spatiotemporal MNNs (1) and (6) achieve PDT synchronization under the controller (25).

Proof. The Lyapunov functional can be chosen as:

$$V(t) = \int_\Gamma \sum_{\ell=1}^{p} e_\ell^2(t,\rho) \mathrm{d}\rho. \tag{26}$$

When $t \in [t_\chi, s_\chi)$, the Dini derivative of $V(t)$ along the system (13) as

$$\begin{aligned} D^+V(t) = & \int_\Gamma \Big\{ \sum_{\ell=1}^{p} 2e_\ell(t,\rho) \Big[\sum_{k=1}^{l} d_{\ell k} \frac{\partial^2 e_\ell(t,\rho)}{\partial \rho_k^2} \\ & - c_\ell e_\ell(t,\rho) + \sum_{n=1}^{p} \underline{a}_{\ell n} [f_n(\tilde{z}_n(t,\rho)) \\ & - f_n(z_n(t,\rho))] + \sum_{n=1}^{p} [\underline{a}_{\ell n} - \bar{a}_{\ell n}] f_n(z_n(t,\rho)) \\ & - \kappa_\ell sign(e_\ell(t,\rho)) - \frac{T_0}{T_c} \alpha_\ell \hat{e}^{-1}(t) e_\ell(t,\rho) \\ & - \frac{T_0}{T_c} \beta_\ell \hat{e}^{2(q-1)}(t) e_\ell(t,\rho) \Big] \Big\} \mathrm{d}\rho, \end{aligned} \tag{27}$$

$$\begin{aligned} \leq & \int_\Gamma \Big\{ \sum_{\ell=1}^{p} \sum_{k=1}^{l} 2e_\ell(t,\rho) d_{\ell k} \frac{\partial^2 e_\ell(t,\rho)}{\partial \rho_k^2} \\ & - \sum_{\ell=1}^{p} 2c_\ell e_\ell^2(t,\rho) + \sum_{\ell=1}^{p} \sum_{n=1}^{p} 2e_\ell(t,\rho) \underline{a}_{\ell n} g_n(e_n(t,\rho)) \\ & + \sum_{\ell=1}^{p} \sum_{n=1}^{p} 2d_{\ell n}^a F_n |e_\ell(t,\rho)| - \sum_{\ell=1}^{p} 2\kappa_\ell |e_\ell(t,\rho)| \Big\} \mathrm{d}\rho \\ & - \frac{2T_0}{T_c} \int_\Gamma \sum_{\ell=1}^{p} \alpha_\ell e_\ell(t,\rho) \hat{e}^{-1}(t) e_\ell(t,\rho) \mathrm{d}\rho \\ & - \frac{2T_0}{T_c} \int_\Gamma \sum_{\ell=1}^{p} \beta_\ell e_\ell(t,\rho) \hat{e}^{2(q-1)}(t) e_\ell(t,\rho) \mathrm{d}\rho. \end{aligned}$$

Similar to the proof in Theorem 1, from the definition

of $\hat{e}(t)$, one has

$$\begin{aligned}
&-\frac{2T_0}{T_c}\int_\Gamma\sum_{\ell=1}^{p}\alpha_\ell e_\ell(t,\rho)\hat{e}^{-1}(t)e_\ell(t,\rho)\mathrm{d}\rho\\
&=-\frac{2T_0}{T_c}\hat{e}^{-1}(t)\int_\Gamma\sum_{\ell=1}^{p}\alpha_\ell e_\ell^2(t,\rho)\mathrm{d}\rho\\
&\le-\frac{2T_0}{T_c}\min_{1\le\ell\le p}\{\alpha_\ell\}\,\hat{e}^{-1}(t)\hat{e}^2(t)\\
&=-\frac{2T_0}{T_c}\min_{1\le\ell\le p}\{\alpha_\ell\}\,V^{\frac{1}{2}}(t),
\end{aligned}\tag{28}$$

$$\begin{aligned}
&-\frac{2T_0}{T_c}\int_\Gamma\sum_{\ell=1}^{p}\beta_\ell e_\ell(t,\rho)\hat{e}^{2(q-1)}(t)e_\ell(t,\rho)\mathrm{d}\rho\\
&=-\frac{2T_0}{T_c}\hat{e}^{2(q-1)}(t)\int_\Gamma\sum_{\ell=1}^{p}\beta_\ell e_\ell^2(t,\rho)\mathrm{d}\rho\\
&\le\frac{2T_0}{T_c}\min_{1\le\ell\le p}\{\beta_\ell\}\,\hat{e}^{2(q-1)}(t)\hat{e}^2(t)\\
&=-\frac{2T_0}{T_c}\min_{1\le\ell\le p}\{\beta_\ell\}\,V^{q}(t).
\end{aligned}\tag{29}$$

Substituting Eqs (18)-(19) and (28)-(29), one derives

$$\begin{aligned}
D^+V(t)\le&\int_\Gamma\sum_{\ell=1}^{p}\Big[-\zeta_\ell-2c_\ell+\sum_{n=1}^{p}(|\underline{a}_{\ell n}|l_n+|\underline{a}_{n\ell}|l_\ell)\Big]\\
&\times e_\ell^2(t,\rho)\mathrm{d}\rho-\frac{2T_0}{T_c}\min_{1\le\ell\le p}\{\alpha_\ell\}\,V^{\frac{1}{2}}(t)\\
&+\int_\Gamma\Big(\sum_{\ell=1}^{p}2(\sum_{n=1}^{p}d_{\ell n}^aF_n-\kappa_\ell)\Big)|e_\ell(t,\rho)|\mathrm{d}\rho\\
&-\frac{2T_0}{T_c}\min_{1\le\ell\le p}\{\beta_\ell\}\,V^{q}(t)\\
\le&NV(t)-\frac{T_0}{T_c}\lambda V^{\mu}(t)-\frac{T_0}{T_c}\gamma V^{\nu}(t).
\end{aligned}\tag{30}$$

When $t\in[s_\chi,t_{\chi+1})$, one has

$$\begin{aligned}
D^+V(t)\le&\int_\Gamma\sum_{\ell=1}^{p}\Big[-\zeta_\ell-2c_\ell+\sum_{n=1}^{p}(|\underline{a}_{\ell n}|l_n+|\underline{a}_{n\ell}|l_\ell)\Big]\\
&\times e_\ell^2(t,\rho)\mathrm{d}\rho+\int_\Gamma\Big(\sum_{\ell=1}^{p}2(\sum_{n=1}^{p}d_{\ell n}^aF_n-\kappa_\ell)\Big)|e_\ell(t,\rho)|\mathrm{d}\rho\\
\le&NV(t).
\end{aligned}\tag{31}$$

Combining (30) and (31), it follows that

$$\dot{V}(t)\le\begin{cases}k_1V(t)-\frac{T_0}{T_c}\lambda V^{\mu}(t)-\frac{T_0}{T_c}\gamma V^{\nu}(t), & t\in[t_\chi,s_\chi),\\ k_2V(t), & t\in[s_\chi,t_{\chi+1}),\end{cases}\tag{32}$$

Here, $k_1=k_2=N=\max\limits_{1\le\ell\le p}\{N_\ell\}$, $\mu=q>1$, $\nu=\frac{1}{2}$, $\gamma=2\min\limits_{1\le\ell\le p}\{\alpha_\ell\}$, and $\lambda=2\min\limits_{1\le\ell\le p}\{\beta_\ell\}$. Therefore, according to Lemma 3, the systems (1) and (6) achieve PDT synchronization.

Table 1. Parameter value

parameter	Value	parameter	Value
$d_{\ell k}$	0.1	h_k	5
c_ℓ	0.94	α_ℓ	1.2
β_ℓ	1.3	$\hat{a}_{11}$	2.128
$\hat{a}_{12}$	-1.224	$\hat{a}_{13}$	-1.124
$\hat{a}_{21}$	-1.224	$\hat{a}_{22}$	1.152
$\hat{a}_{23}$	-7.808	$\hat{a}_{31}$	-1.224
$\hat{a}_{32}$	10.347	$\hat{a}_{33}$	2.320
$\check{a}_{11}$	-1.224	$\check{a}_{12}$	-1.224
$\check{a}_{13}$	-1.124	$\check{a}_{21}$	-2.224
$\check{a}_{22}$	2.152	$\check{a}_{23}$	-9.808
$\check{a}_{31}$	-1.224	$\check{a}_{32}$	9.447
$\check{a}_{33}$	1.320	κ_ℓ	0.2
q	2.3	φ	0.2
l_ℓ	0.2	$\eta_1(\rho)$	0.2
$\eta_2(\rho)$	0.5	$\eta_3(\rho)$	0.7

4 Numerical examples and simulations

In this section, the accuracy of the conclusions of the previous section is verified through an example.

Example 1 For $l=3$, consider following spatiotemporal MNNs

$$\begin{aligned}
\frac{\partial z_\ell(t,\rho)}{\partial t}=&\sum_{k=1}^{3}d_{\ell k}\frac{\partial^2 z_\ell(t,\rho)}{\partial\rho_k^2}-c_\ell z_\ell(t,\rho)\\
&+\sum_{n=1}^{3}a_{\ell n}f_n\left(z_n(t,\rho)\right)+I_\ell,
\end{aligned}\tag{33}$$

$$\begin{aligned}
\frac{\partial \tilde{z}_\ell(t,\rho)}{\partial t}=&\sum_{k=1}^{3}d_{\ell k}\frac{\partial^2 \tilde{z}_\ell(t,\rho)}{\partial\rho_k^2}-c_\ell \tilde{z}_\ell(t,\rho)\\
&+\sum_{n=1}^{3}a_{\ell n}f_n\left(\tilde{z}_n(t,\rho)\right)+I_\ell+u_\ell(t,\rho),
\end{aligned}\tag{34}$$

where $f_n(r)=\tanh(r)$. The values of the parameters are as shown in Table 1.

The spatiotemporal evolution of system (4) are shown in Figures 1, 2, and 3. Since $\lambda=2.6$, $\gamma=2.4$, $N=0.2552$, according to Theorem 1, the systems (33) and (34) achieve FXT synchronization via controller (14), with an estimated ST of $T^*=4.9266$. The numerical simulation results are shown in Figures 4, 5, and 6.

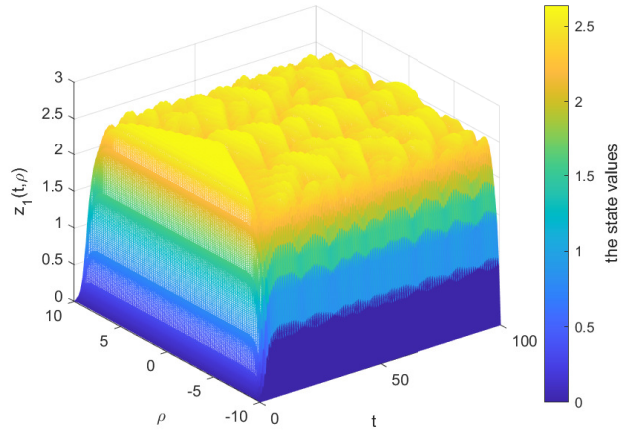

Figure 1. Evolution of the state $z_1(t,\rho)$ in system (33).

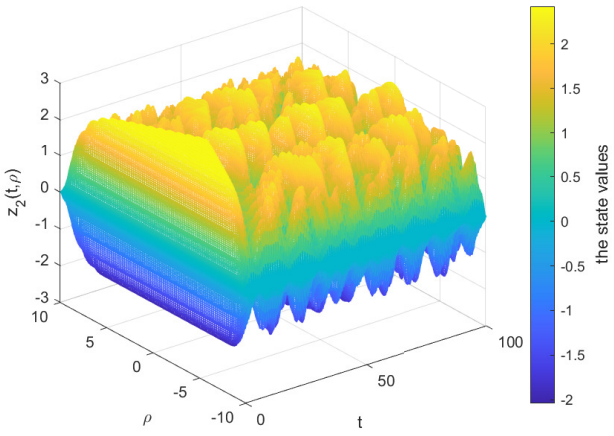

Figure 2. Evolution of the state $z_2(t,\rho)$ in system (33).

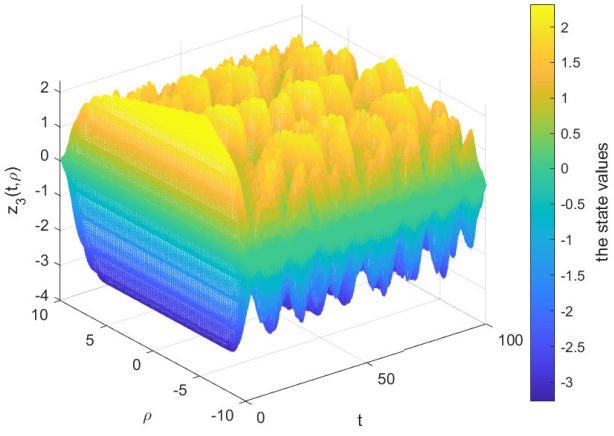

Figure 3. Evolution of the state $z_3(t,\rho)$ in system (33).

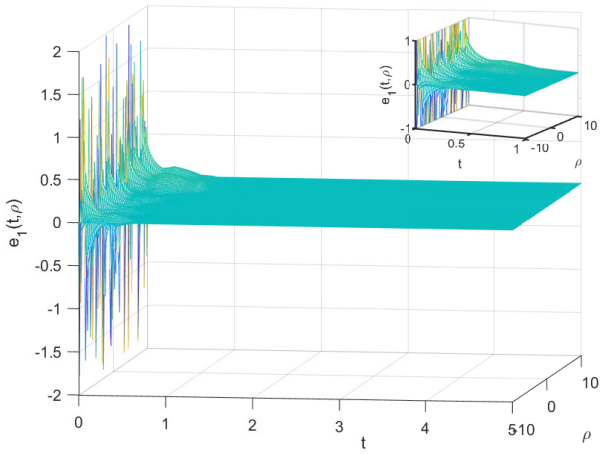

Figure 4. Time evaluation of synchronization error $e_1(t,\rho)$.

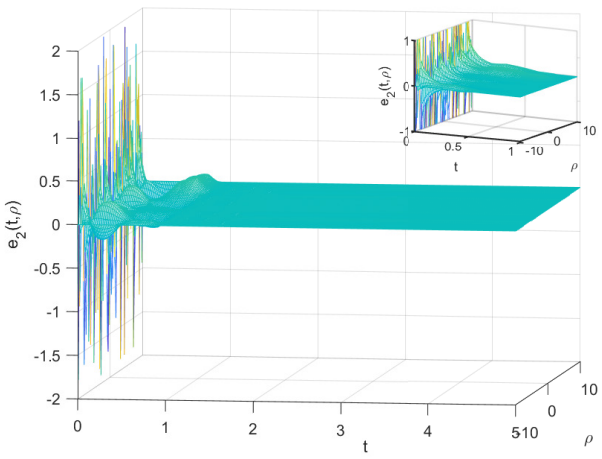

Figure 5. Time evaluation of synchronization error $e_2(t,\rho)$.

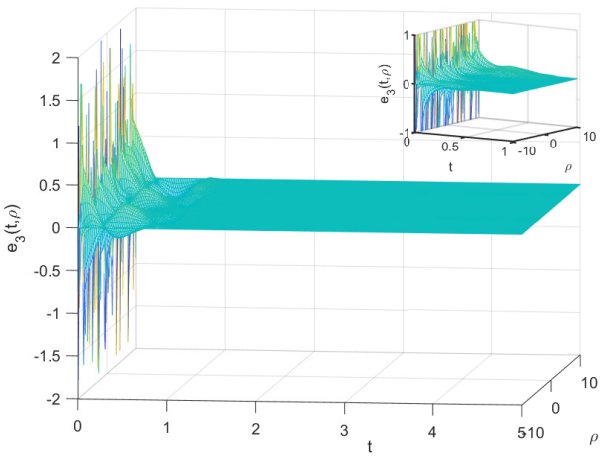

Figure 6. Time evaluation of synchronization error $e_3(t,\rho)$.

Now we consider the PDT synchronization between systems (33) and (34) under controller (25). By calculating $T_0 = 5.663$ and selecting $T_c = 4.512$, $\frac{T_0}{T_c}\lambda = 3.2633$, $\frac{T_0}{T_c}\gamma = 3.0122$, $N = 0.2552$, so the conditions in Theorem 2 are satisfied. Therefore, according to Theorem 2, the drive-response systems (33) and (34) achieve PDT synchronization. The prescribed time $T_c = 4.512$ is less than $T_0 = 5.663$ and $T^* = 4.9266$. The numerical simulation results are shown in Figures 7, 8, and 9.

Table 2. Comparison of AIC, ETC, and SDC.

Feature	ASIC	ETC	SDC
Trigger Mechanism	Time-based(flexible)	Event-based(error-dependent)	Time-based(fixed)
Energy Consumption	Low(intermittent)	Very low(sparse updates)	Moderate(periodic)
Implementation Complexity	Low	High(requires monitoring)	Moderate
Adaptability	High(aperiodic)	High(dynamic)	Low(fixed period)
Conservativeness	Moderate	Low(efficient triggering)	High(fixed intervals)
Suitability	High	Moderate	Moderate

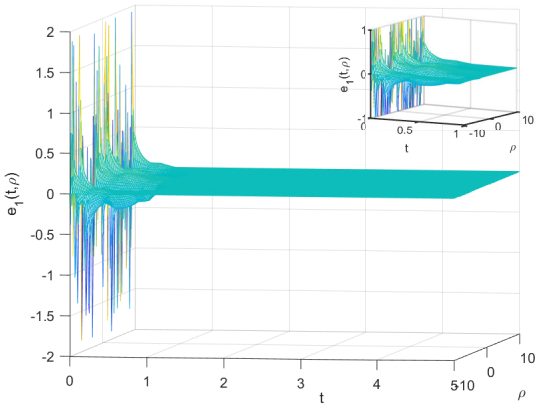

Figure 7. Time evaluation of synchronization error $e_1(t,\rho)$.

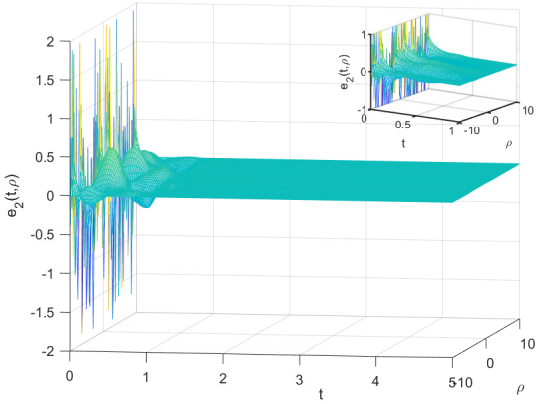

Figure 8. Time evaluation of synchronization error $e_2(t,\rho)$.

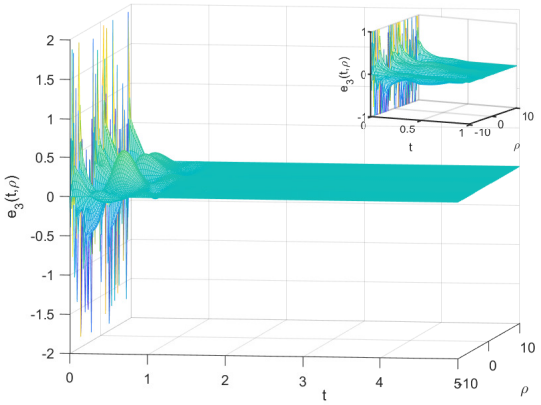

Figure 9. Time evaluation of synchronization error $e_3(t,\rho)$.

Remark 4. The comparisons of the features of ASIC, event-triggered control (ETC), and sampled-data control (SDC) are presented in Table 2.

5 Conclusion

This paper investigates the FXT/PDT synchronization issues of spatiotemporal MNNs. First, a novel ASIC is introduced to tackle the challenge caused by the switching behaviour of memristor. Second, under the newly ASIC control protocol, Guass's divergence theorem and the Lyapunov functional method are utilized to study the FXT/PDT synchronization of MNNs. The paper concludes with the validation of theoretical findings through a numerical simulation. Furthermore, unlike time-based intermittent control, event-based intermittent control determines the transition between the active and idle phases of the controller based on the dynamic evolution of the system, thereby further conserving communication resources. In our future research, we will explore the event-triggered ASIC mechanisms to achieve FXT/PDT synchronization of spatiotemporal MNNs.

Data Availability Statement

Data will be made available on request.

Funding

This work was supported the Outstanding Youth Program of Xinjiang, China under Grant 2022D01E10 and the National Natural Science Foundation of China under Grant 62266042.

Conflicts of Interest

The authors declare no conflicts of interest.

Ethical Approval and Consent to Participate

Not applicable.

References

[1] Shi, B., Bai, X., & Yao, C. (2016). An end-to-end trainable neural network for image-based sequence recognition and its application to scene text recognition. *IEEE Transactions on Pattern Analysis and Machine Intelligence, 39*(11), 2298–2304. [CrossRef]

[2] AL-Masri, A. N., Ab Kadir, M. Z. A., Hizam, H., & Mariun, N. (2013). A novel implementation for generator rotor angle stability prediction using an adaptive artificial neural network application for dynamic security assessment. *IEEE Transactions on Power Systems, 28*(3), 2516–2525. [CrossRef]

[3] Cheng, J., Liang, L., Yan, H., Cao, J., Tang, S., & Shi, K. (2022). Proportional-integral observer-based state estimation for Markov memristive neural networks with sensor saturations. *IEEE Transactions on Neural Networks and Learning Systems, 35*(1), 405–416. [CrossRef]

[4] Shanmugam, L., Mani, P., Rajan, R., & Joo, Y. H. (2018). Adaptive synchronization of reaction–diffusion neural networks and its application to secure communication. *IEEE Transactions on Cybernetics, 50*(3), 911–922. [CrossRef]

[5] Qin, Z., Wang, J. L., Wang, Q., Dai, L. J., & Guo, X. Y. (2019). Passivity and synchronization of coupled reaction–diffusion neural networks with multiple coupling and uncertain inner coupling matrices. *Neurocomputing, 341*, 26–40. [CrossRef]

[6] Yang, X., Cao, J., & Yang, Z. (2013). Synchronization of coupled reaction-diffusion neural networks with time-varying delays via pinning-impulsive controller. *SIAM Journal on Control and Optimization, 51*(5), 3486–3510. [CrossRef]

[7] Cao, Y., Cao, Y., Guo, Z., Huang, T., & Wen, S. (2020). Global exponential synchronization of delayed memristive neural networks with reaction–diffusion terms. *Neural Networks, 123*, 70–81. [CrossRef]

[8] Chua, L. (2003). Memristor-the missing circuit element. *IEEE Transactions on Circuit Theory, 18*(5), 507–519. [CrossRef]

[9] Adhikari, S. P., Yang, C., Kim, H., & Chua, L. O. (2012). Memristor bridge synapse-based neural network and its learning. *IEEE Transactions on Neural Networks and Learning Systems, 23*(9), 1426–1435. [CrossRef]

[10] Hu, X., Feng, G., Duan, S., & Liu, L. (2016). A memristive multilayer cellular neural network with applications to image processing. *IEEE Transactions on Neural Networks and Learning Systems, 28*(8), 1889–1901. [CrossRef]

[11] Hu, X., Duan, S., & Wang, L. (2012). A novel chaotic neural network using memristive synapse with applications in associative memory. *Abstract and Applied Analysis, 1*, 405739. [CrossRef]

[12] Galicki, M. (2015). Finite-time control of robotic manipulators. *Automatica, 51*, 49–54. [CrossRef]

[13] Du, H., Li, S., & Qian, C. (2011). Finite-time attitude tracking control of spacecraft with application to attitude synchronization. *IEEE Transactions on Automatic Control, 56*(11), 2711–2717. [CrossRef]

[14] Zhang, X., Zhou, W., Karimi, H. R., & Sun, Y. (2020). Finite-and fixed-time cluster synchronization of nonlinearly coupled delayed neural networks via pinning control. *IEEE Transactions on Neural Networks and Learning Systems, 32*(11), 5222–5231. [CrossRef]

[15] Polyakov, A. (2011). Nonlinear feedback design for fixed-time stabilization of linear control systems. *IEEE Transactions on Automatic Control, 57*(8), 2106–2110. [CrossRef]

[16] Hu, C., & Jiang, H. (2021). Special functions-based fixed-time estimation and stabilization for dynamic systems. *IEEE Transactions on Systems, Man, and Cybernetics: Systems, 52*(5), 3251–3262. [CrossRef]

[17] Hu, C., He, H., & Jiang, H. (2020). Fixed/preassigned-time synchronization of complex networks via improving fixed-time stability. *IEEE Transactions on Cybernetics, 51*(6), 2882–2892. [CrossRef]

[18] Kong, F., Ni, H., Zhu, Q., Hu, C., & Huang, T. (2023). Fixed-time and predefined-time synchronization of discontinuous neutral-type competitive networks via non-chattering adaptive control strategy. *IEEE Transactions on Network Science and Engineering, 10*(6), 3644–3657. [CrossRef]

[19] Zhang, G., & Cao, J. (2023). New results on fixed/predefined-time synchronization of delayed fuzzy inertial discontinuous neural networks: Non-reduced order approach. *Applied Mathematics and Computation, 440*, 127671. [CrossRef]

[20] Abdurahman, A., Abudusaimaiti, M., & Jiang, H. (2023). Fixed/predefined-time lag synchronization of complex-valued BAM neural networks with stochastic perturbations. *Applied Mathematics and Computation, 444*, 127811. [CrossRef]

[21] Wang, S., Guo, Z., Wen, S., Huang, T., & Gong, S. (2020). Finite/fixed-time synchronization of delayed memristive reaction-diffusion neural networks. *Neurocomputing, 375*, 1–8. [CrossRef]

[22] Hu, C., Jiang, H., & Teng, Z. (2009). Impulsive control and synchronization for delayed neural networks with reaction–diffusion terms. *IEEE Transactions on Neural Networks, 21*(1), 67–81. [CrossRef]

[23] Yu, Z., Yu, S., & Jiang, H. (2023). Finite/fixed-time event-triggered aperiodic intermittent control for nonlinear systems. *Chaos, Solitons & Fractals, 173*, 113735. [CrossRef]

[24] Zhao, C., Zhong, S., Zhang, X., Zhong, Q., & Shi, K. (2020). Novel results on nonfragile sampled-data exponential synchronization for delayed complex dynamical networks. *International Journal of Robust and Nonlinear Control, 30*(10), 4022–4042. [CrossRef]

[25] Abudireman, A., Abdurahman, A., & Jiang, H.

(2025). Fixed-time synchronization of spatiotemporal Cohen-Grossberg neural networks via aperiodic intermittent control. *Communications in Nonlinear Science and Numerical Simulation*, 108991. [CrossRef]

[26] Qiao, Y., Abudireman, A., & Abudurahman, A. (2025). Aperiodic Intermittent Control Based Predefined-Time Synchronization of Spatiotemporal Neural Networks. In *2025 37th Chinese Control and Decision Conference* (*CCDC*) (pp. 6597–6602). [CrossRef]

[27] Yang, J., Chen, G., Zhu, S., Wen, S., & Hu, J. (2023). Fixed/prescribed-time synchronization of BAM memristive neural networks with time-varying delays via convex analysis. *Neural Networks, 163*, 53–63. [CrossRef]

[28] Pu, H., & Li, F. (2023). Fixed-time projective synchronization of delayed memristive neural networks via aperiodically semi-intermittent switching control. *ISA Transactions, 133*, 302–316. [CrossRef]

[29] Lu, J. G. (2008). Global exponential stability and periodicity of reaction–diffusion delayed recurrent neural networks with Dirichlet boundary conditions. *Chaos, Solitons & Fractals, 35*(1), 116–125. [CrossRef]

Ying Qiao received the B.S. degree in mathematics and applied mathematics from the School of Mathematics and information science, Zhongyuan University of Technology, Zhengzhou, China, in 2021. Currently, she is working towards the M.S. degree at Xinjiang University, and her current research interests include stability analysis and synchronization control of impulsive systems and neural networks. (Email: 2776883628@qq.com)

Aminamuhan Abudireman received the B.S. degree in mathematics and applied mathematics in 2022, and the M.S. degree in applied mathematics in 2025 from the College of Mathematics and System Sciences, Xinjiang University, Xinjiang, China. Her current research interests include stability analysis and synchronization control of reaction-diffusion neural networks. (Email: aminamuhan@163.com)

Abdujelil Abdurahman received the B.S. degree in mathematics and applied mathematics in 2010, the M.S. degree in control theory in 2013 and the Ph.D. degree in applied mathematics in 2016 from the College of Mathematics and System Sciences, Xinjiang University, Xinjiang, China. He is currently a Professor and Doctoral Advisor of Mathematics and System Science with Xinjiang University. His current research interests include neural networks, complex networks, nonsmooth analysis and image processing. (Email: abdujelil@xju.edu.cn)

Jingjing You received the B.S. degree in mathematics and applied mathematics from the College of Mathematics and Statistics, Shangqiu Normal University, Shangqiu, China, in 2019. In 2023, she received the M.S. degree in operations research and control theory from Xinjiang University, Xinjiang, China. Currently, she is working towards the Ph.D. degree at Xinjiang University, and her current research interests include stability analysis and synchronization control of stochastic systems and complex networks. (Email: yjjxju@163.com)